Hindawi Publishing Corporation
Journal of Metallurgy
Volume 2014, Article ID 248542, 10 pages
http://dx.doi.org/10.1155/2014/248542

Research Article

Aluminium AA6061 Matrix Composite Reinforced with Spherical Alumina Particles Produced by Infiltration: Perspective on Aerospace Applications

Claudio Bacciarini[1,2] and Vincent Mathier[1]

[1] *Constellium Innovation Cells, EPFL-Innovation Park, Bâtiment E, 1015 Lausanne, Switzerland*
[2] *JetSolutions SA, Route de Montena 89, 1728 Rossens, Switzerland*

Correspondence should be addressed to Claudio Bacciarini; claudio.bacciarini@gmail.com

Received 24 August 2014; Accepted 6 November 2014; Published 30 November 2014

Academic Editor: Sunghak Lee

Metal matrix composites, based on AA6061 reinforced with 60 vol% Al_2O_3 spherical particles, were produced by gas pressure infiltration and characterized for hardness, impulse excitation modulus, tensile properties (at room temperature and at 250°C), and machining. It was experimentally demonstrated that the novel alumina powder used in the present work does not react with the liquid Mg-containing matrix during the infiltration process. The AA6061 matrix therefore retains its ability to be strengthened by precipitation heat treatment. The latter behaviour combined with the spherical particle shape confers the studied material higher strength and better machinability in comparison with similar composites produced using standard angular alumina particles. The overall features are promising for applications in the aerospace industry, where light and strong materials are required.

1. Introduction

Metal matrix composites (MMCs) have generated interest in academia and industry for more than four decades because of the possibility to tailor their physical and mechanical properties. According to [1] the global production of aluminium MMCs was 2700 metric tons in 2008. Figure 1 illustrates the dominance of ground transportation (mostly automotive) in terms of the produced volume of these materials. Due to high production rate requirements of the automotive industry, the preferred production methods in this segment are cost-effective squeeze-casting or pressure die-casting processes [2], which enable the material cost to be low enough for adoption by car manufacturers in real applications.

From a market value perspective, a remarkable 56% is captured by the electronics segment. The increasing importance of wireless communication and increasing power of microprocessors make electronics cooling of vital importance, typically to extend the lifetime and to allow integration in plastic housings (e.g., handset devices). The ability to tailor the coefficient of thermal expansion (CTE) and thermal conductivity has brought a real step change in designing electronics, driving the use of MMCs in this application. According to Mortensen [2], the preferred manufacturing process in this case is gas pressure infiltration because complexity and accuracy are required.

Aerospace applications represent 11% of the value. Composites for this industry are mainly processed by powder metallurgy, habitually followed by hot working, that is, forging, extrusion or rolling [1, 3]. In this case MMCs are used for parts that require high stiffness or high strength together with wear and fatigue resistance. In addition, other properties like toughness, corrosion resistance, or creep resistance (for warm and high-temperature applications) must meet required standards.

Aerospace manufacturers are constantly looking for lightweighting in order to reduce the fuel consumption. Every kg saved on a commercial aircraft corresponds to 700$ [1] saved for the airlines (whilst, for instance, the figure is 7$ for every kg saved, in the automotive sector); aluminium MMCs are therefore good candidates to further decrease these costs and turn aviation into a greener business.

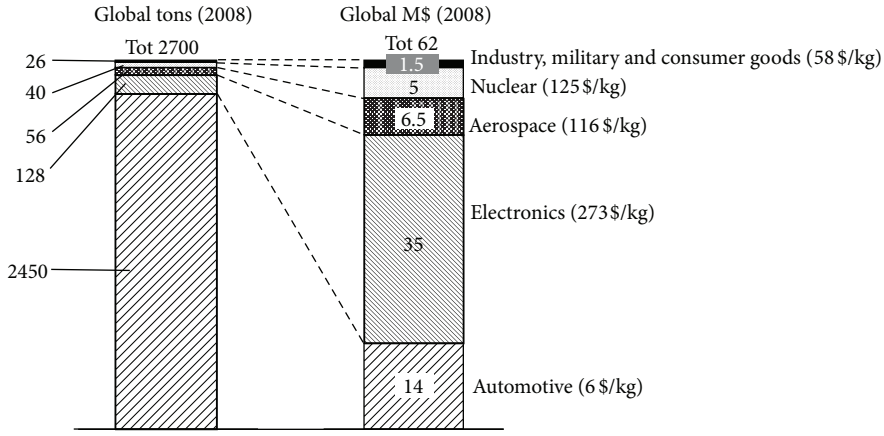

Figure 1: Global mass and value distribution amongst the main market segments for aluminium MMCs. Based on data from [1].

The work presented in this paper addresses the mechanical and machining properties of an aluminium-based MMC reinforced with 60% volume fraction of spherical alumina particles. Its microstructure is shown in Figure 2. The composite of this work is obtained by gas pressure infiltration of an AA6061 alloy into a preform of packed spherical Al_2O_3 particles. The gas infiltration process allows producing highly reinforced, defect-free composites with the possibility to produce near-net shape components, and this potentially at lower production cost than using the powder metallurgy route. Angular alpha alumina, which is originally produced for abrasive products, has been and still is widely used for particle reinforced MMC (PRMMC) fabrication. This kind of powder is produced by comminution, which results in very sharp particles. A portion of these particles even contains cracks. When introduced into a metal matrix the result is a brittle composite [4]. In addition to that, during the composite processing (be it by squeeze casting, infiltration, or powder metallurgy), alpha alumina reacts with the magnesium contained in the present matrix alloy by forming a spinel $MgAl_2O_4$phase at the matrix/particle interface. This reaction removes the Mg from the alloy [5, 6, 8]. This latter phenomenon reduces or cancels the strengthening effect obtained in the matrix through Mg-based precipitation. In addition, according to [6, 7], an embrittlement of the composite can occur due to the presence of this spinel phase. For all these reasons, the use of abrasive grade alpha Al_2O_3 powder as a reinforcement is not optimal.

The choice of the reinforcement powder in the present paper has thus been driven by two main aspects: the nature of the alumina and the shape of the particles. The spherical ceramic powder selected here is produced and provided by GAP Engineering LLC based in Ash Grove, MO. As reported by Harrigan [8], this powder is an alpha alumina which has been modified into a mixed alpha-gamma-amorphous alumina. Its particularity is that during sintering it does not react with Mg additions to aluminium, thus retaining the strengthening effect in a matrix like AA6061 after precipitation heat treatment [9].

Composites of aluminium alloys reinforced with such spherical alumina particles are now produced commercially by powder metallurgy; they have attractive mechanical properties coupled with superior machinability compared with other particle reinforced aluminium composites [8, 9]. In work to date, the volume fraction of spherical particles has been kept in the range from 5 to 20%. Here, we explore significantly higher fractions ceramic, close to 60%. We do so by producing the composites by pressure infiltration, a process relying on flow of the matrix in a liquid state, which is better suited than powder metallurgy to the production of highly particle reinforced metal matrix composites [2]. This processing method will allow confirming whether or not the GAP alumina powder remains inert when facing, in the present case, an Mg-containing alloy in liquid form.

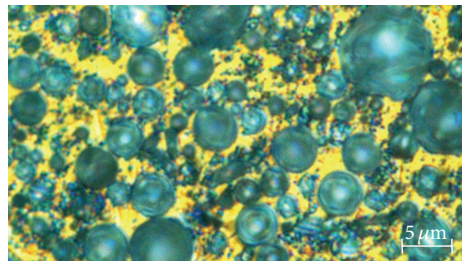

Figure 2: Microstructure of spherical PRMMC.

2. Material Processing

Main characteristics of the GAP spherical alumina particles employed for the production of composites of this work are given in Table 1. In addition to GAP powder, Alodur angular alpha alumina powder, produced by Treibacher Schleifmittel in Laufenburg, Germany, was also infiltrated for comparison purposes. This powder, of grit size F600, has almost the same particle size as the GAP powder, in Table 1. Note also the difference in density between the two types of alumina, which gives a significant advantage to the lighter GAP powder, as discussed in Section 4.

Both composites have been processed as described in [2] using a laboratory gas pressure infiltration device. The

Table 1: Main features of produced spherical and angular particle MMCs.

Composite designation	Spherical PRMMC	Angular PRMMC
Matrix	AA6061	AA6061
Reinforcement type	α-γ-Amorphous Al_2O_3	α-Al_2O_3
Reinforcement shape	Spherical	Angular
Reinforcement density [g/cm^3]	3.75*	3.95**
Particle size [μm]		
D3	31	19
D50	6.5	9.3
D94	2	3
Volume fraction of reinforcement (V_f)	0.6	0.6

*Source: GAP Engineering, measured by University of Missouri. **Source: Treibacher Schleifmittel product datasheet.

molten AA6061 alloy was pushed into the alumina preform with an argon gas pressure of 6 MPa and then directionally solidified thanks to a copper chill at his bottom. The resulting billets are 36 mm in diameter and 110 mm in length. After infiltration the billets were then heat-treated to T4 (solution heat treatment 530°C during 2 hours followed by water quench), T6 (T4 followed by precipitation heat treatment 160°C during 18 hours), and O (annealing treatment 415°C during 3 hours followed by cooling at 0.4°C/min till 260°C) tempers. Composites with sieved GAP powder have also been processed in order to observe eventual improvements on mechanical properties and machining. The sieving is obtained by letting the powder vibrate and fall through 20 μm and 10 μm grit sieves. Thus two powder batches could be produced, one with particles size <10 μm and another with particle size <20 μm.

3. Testing

3.1. Mechanical Testing. Vickers hardness testing was carried out on a Brickers-200 machine from Gnehm (Horgen, Switzerland) by applying a 10 kg load during 16 s.

To measure elastic properties an impulse excitation apparatus was employed. The impulsion and the corresponding frequential response were, respectively, induced and captured by a GrindoSonic Mk5-Industrial device (J. W. Lemmens N. V., Leuven, Belgium) following the ASTM E1876 procedure.

Tensile tests were performed on rectangular section dogbone tensile specimens at a nominal strain rate of 3.10^{-5} s^{-1} according to ASTM E8 standard, using a MTS (Minneapolis, USA) Alliance RT/50 universal mechanical testing apparatus. Fractography and EDX mapping of the broken tensile samples were run with a scanning electron microscope (SEM, model FEI XL30-EBSP).

Tensile tests at 250°C were carried out at Liebherr Aerospace in Toulouse, France. In that case the strain rate was 8.10^{-5} s^{-1} in the elastic zone and 8.10^{-4} s^{-1} in the plastic zone in accordance with ASTM E21.

Table 2: Main characteristics of spherical and angular composites.

	Spherical PRMMC 60%	Angular PRMMC 60%
Density [g/cm^3]	3.25	3.34
E [GPa]	150	150
G [GPa]	58	58
Poisson's ratio	0.29	0.29
Hardness at T6 [HV10]	216	159
Hardness at T4 [HV10]	167	165

In order to compare the measured properties to relevant benchmarks, data for commercial Duralcan and Boralcan composites, matrix alloy AA6061, typical aerospace alloy AA2024, and AIRWARE 2196 (new lithium containing aerospace grade alloy) will be displayed on the relevant plots.

3.2. Machining. Preliminary qualitative turning trials were conducted with a machining expert from JRS Tools company (Payerne, Switzerland) in order to identify the right turning parameters and to find the appropriate insert material, geometry, and coating. This specific testing was set up to address one commonly mentioned barrier to the adoption for metal matrix composites, namely, the machining cost (the goal being to use general performance inserts and not expensive diamond cutting tools).

An Al_2O_3+TiC insert (grade HC4) from NTK Cutting Tools (Ratingen, Germany) with a TiN coating and a negative rake angle was selected. Machining trials were carried out on a W570E lathe from Voest-Alpine (Linz, Austria) with the following cutting parameters: cutting speed = 50 m/min, feed = 0.3 mm/rev, cutting depth = 0.5 and 2 mm (see next section), and dry machining. The chosen tool insert geometry as well as the cutting parameters is typical for rough turning, the goal being to reproduce high material removal machining rather than finishing.

Tool insert flank wear measurements and machined surface observation were done after removal of 50 cm^3 of material.

Insert flank wear (VB) measurements were done with a macrocamera capturing pictures of the worn zone and the machined surface was observed with a scanning electron microscope (SEM, model FEI XL30-EBSP).

4. Results

4.1. Mechanical Properties: Hardness and Stiffness. Table 2 shows the measured values and compares the features of the spherical and angular particle reinforced composites. Elastic (E) and shear (G) modulus values are identical whilst the densities are slightly different due to a ~5% density gap between Alodur and GAP alumina particles. This difference becomes very important when calculating the specific bending stiffness, as illustrated in Figure 6. The hardness measurements reveal that precipitation of the hard phase Mg_2Si in

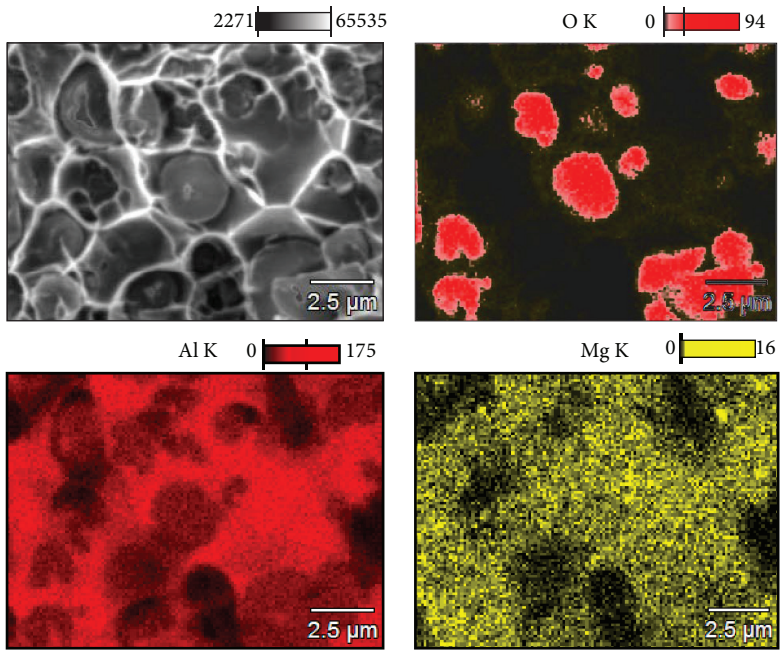

(a)

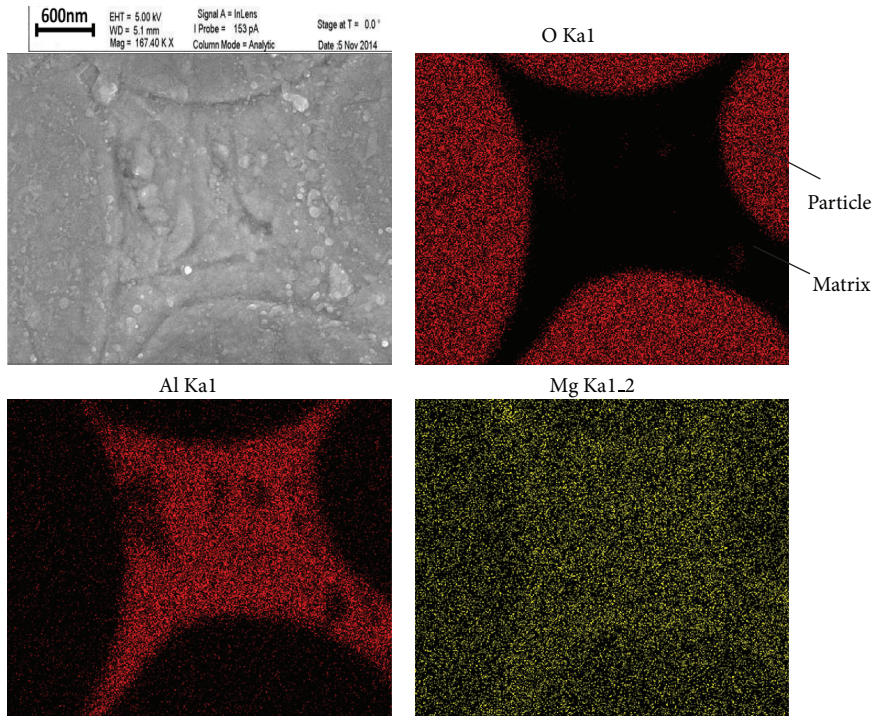

(b)

Figure 3: SEM imaging and EDX mapping for oxygen, aluminium, and magnesium of fracture surface (a) and polished surface (b) done on the spherical PRMMC.

AA6061 matrix does not take place in the angular PRMMC, whereas a strengthening phenomenon brings the hardness from 167HV10 at T4 temper to 216HV10 at T6 temper in the spherical PRMMC. EDX mapping on the fractured surface and on the polished cross section, Figures 3(a) and 3(b), shows that magnesium is homogeneously distributed. No magnesium agglomeration around the particles is observed indicating that reaction between alumina and Mg does not

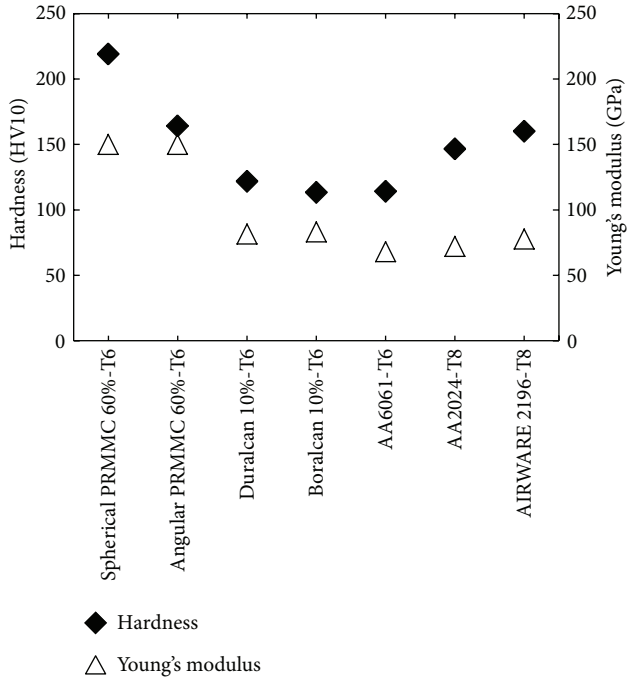

Figure 4: Hardness and elastic modulus comparison between spherical and angular PRMMC, commercial MMCs, reference AA6061 alloy and aerospace alloys AA2024, and AIRWARE 2196. All hardness values: measured. Young's modulus of spherical and angular PRMMC and Boralcan: measured. Young's modulus of Duralcan from [10], AA6061 and AA2024 from [11], and AIRWARE 2196 from Constellium product datasheet.

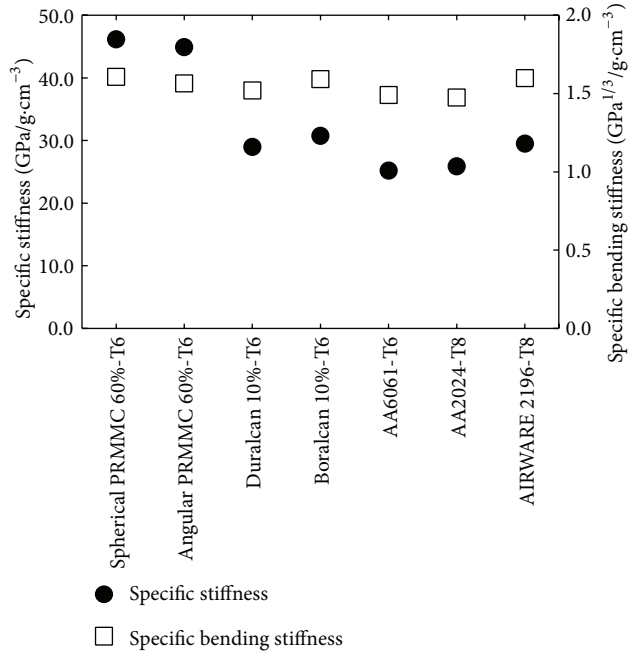

Figure 5: Specific stiffness and specific bending stiffness comparison between spherical and angular PRMMC, commercial MMCs, reference AA6061 alloy and aerospace alloys AA2024, and AIRWARE 2196. Densities for specific stiffness calculation: spherical and angular PRMMC from Table 2, Duralcan from [10], Boralcan from measurements, AA6061 and AA2024 from [12], and AIRWARE 2196 from Constellium product datasheet.

happen, consistent with the heat treatment response, which suggests that Mg stayed in the matrix and was present to form precipitates. These observations confirm findings from [9] proving that the spherical alumina from GAP does not react with Mg. This proves true even in a liquid state process as the infiltration method used in the present work. Therefore, two major advantages of the novel powder can be identified for the spherical PRMMC: (i) Mg stays in the matrix and contributes to strengthen the composite by formation of precipitates, and (ii) formation of the brittle $MgAl_2O_4$ spinel at the particle-matrix interface is avoided.

The high reinforcement volume fraction of spherical PRMMC and angular PRMMC gives the composites an elastic modulus of 150 GPa. This is close to double the stiffness of commercial aluminium composites and alloys (Figure 4). The spherical PRMMC also shows the highest hardness. The combination of these properties makes it a potentially interesting material for structural applications in which low weight is a design target.

In aerospace applications low weight is of vital importance. Therefore, the density of the material has to be taken into account when evaluating its performance. Figure 5 illustrates that the highly reinforced composites have a high specific stiffness (E/ρ); however one also sees how the gap between them and the other materials is rapidly closed when calculating the rigidity in bending mode ($E^{1/3}/\rho$). The latter value is more meaningful as a figure of merit for a material in aerostructures where bending is the typical loading mode.

In order to better describe the differences in bending stiffness plotted in Figure 5 the relative improvement or reduction in bending stiffness versus the reference (unreinforced) alloy AA6061 is represented in Figure 6. The spherical PRMMC is 7.9% stiffer in bending than AA6061 alloy and also 2.9% better than the similarly processed angular particulate composite thanks to the slightly lower density of GAP alumina. That fact places the infiltrated GAP particle reinforced composite in the same range as best-in-class Al-lithium alloy AIRWARE 2196 and Boralcan composite, which contains light B_4C particles ($\rho_{B4C} = 2.52\,g/cm^3$).

4.2. Mechanical Properties: Tensile. Tensile tests have been performed on the spherical alumina particle reinforced MMC, comparing the mechanical properties for different metallurgical states of the matrix: maximizing strength with the T6 temper or maximizing ductility with the O temper. The curves obtained, in Figure 7(a), show a good repeatability, except for variability regarding the elongation at fracture; this is in turn linked to the rather brittle fracture mode of the composite. This brittle behaviour is confirmed by low elongation values in the T6 condition (Table 3) which makes the application of such a material problematic in aerospace. A higher elongation value of 1.35% is obtained when the spherical PRMMC is in O condition. In that case the yield strength

Table 3: Mechanical properties of spherical PRMMC at room temperature (non aged) and at 250°C after 1000 h ageing at 250°C.

Test temperature [°C]	Temper	YS [MPa]		UTS [MPa]		El. [%]		E [GPa]
		Average	Maximum	Average	Maximum	Average	Maximum	
25	T6	413	415	447	457	0.44	0.55	150 ± 8
25	O	238	239	330	337	1.25	1.35	150 ± 8
250	T6	195	201	210	217	2.50	2.70	105 ± 7

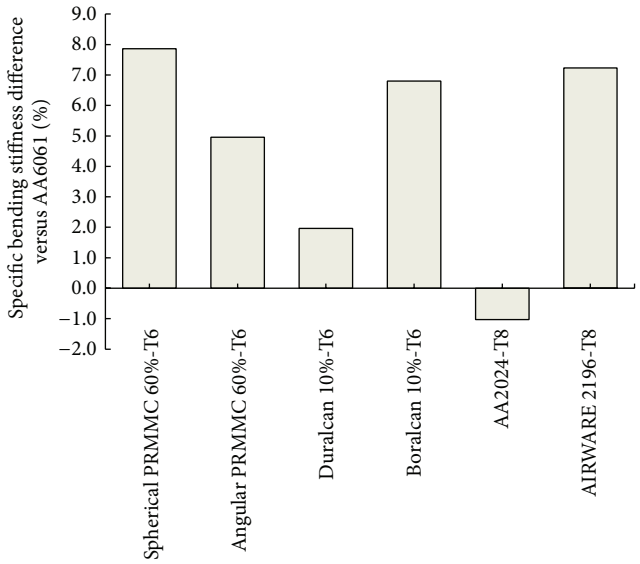

Figure 6: Bending stiffness difference relative to unreinforced AA6061 reference alloy.

(YS) and ultimate tensile strength (UTS) are 238 MPa and 330 MPa, respectively. A rule of thumb for aerospace materials is to have YS above 300 MPa with an elongation above 1%. The present composite does not meet this requirement yet is sufficiently close to warrant an exploration of its thermomechanical postprocessing in future work.

The use of smaller size GAP powder particles to enhance elongation has been attempted by producing composites with sieved reinforcement (all particles <10 μm or <20 μm in size). These variants did not show significant difference in tensile properties, sieving to such sizes thus being ineffective for static properties. Control of particles size is however expected to be more beneficial for fatigue resistance by postponing the crack initiation and decreasing the frequency of particle fracture during crack propagation [13, 14]. Additionally, a smaller particle size in high reinforced composites reduces strain-rate sensitivity and damage accumulation during dynamic compression and therefore is potentially beneficial for post-processing like forging [15, 16].

Further measurements were performed in collaboration with Liebherr Aerospace in Toulouse, France. The spherical PRMMC was exposed to 250°C during 1000 h with subsequent tensile testing at 250°C. In those conditions YS and UTS drop to 195 and 210 MPa, respectively, and the elongation reaches a value of 2.7%. The influence of high reinforcement volume fraction is significant and beneficial when comparing yield strength of AA6061 matrix alloy with spherical PRMMC at 250°C. This is illustrated in Figure 7(b), which also includes curves of current high-temperature aluminium alloys AA2618 and AA2219. The spherical PRMMC shows the highest yield strength value at 250°C. This confirms its potential for warm/hot applications.

These values can be interpreted as a further step in "softening" the matrix to obtain higher elongations and show that the value of 2.7% can be physically reached for such highly reinforced material provided its matrix has adequate properties.

SEM observation of the fracture surfaces reveals that the tested composite is free of broken or cracked particles (Figure 8). Most particles stay embedded in the matrix after fracture. This suggests the presence of a rather healthy interface (no porosity, no microcracks, and no spinel phase). Final material separation happens to a large extent through the thin interparticle matrix bridges.

Strong particles and defect-free interfaces combined with the spherical shape thus allow such high reinforced composite to show an interesting balance of strength and ductility. Improvements of the matrix by applying adequate treatments or tuning its composition can strengthen the network of interparticle bridges and allow the properties of the MMC to match the requirements for aerospace applications.

4.3. Machining. To be used in an actual application, the aptitude of the material to be shaped is an important factor. Powder metallurgy composites reinforced with GAP powder at lower loadings than in the present work have been tested for machining properties by Harrigan [9], showing significant improvements in tool life compared to equivalent SiC composites. This observation was made on 15% reinforced composites, using TiN coated tungsten carbide inserts.

The same procedure was employed in this work in order to evaluate the wear of the tool insert when machining the 60 vol% GAP powder reinforced composite. Figure 9 shows that the highly reinforced spherical PRMMC wears dramatically the tool insert, mainly by two modes: flank wear and cratering. Flank wear cannot by definition be avoided, while cratering typically appears when machining abrasive materials.

The first round of trials (Figure 9(b)) using a cutting depth of 0.5 mm resulted in a flank wear (VB) of 1.15 mm. This is almost four times higher than the threshold value of 0.3 mm. Above this threshold value the tool insert is considered to be no longer usable [17]. By increasing the cutting depth to 2 mm, the insert flank wear value decreased to reach 0.8 mm. This result, obtained through a selection of machining conditions in addition to the spherical shape of the particles [9], brings the spherical PRMMC into the wear

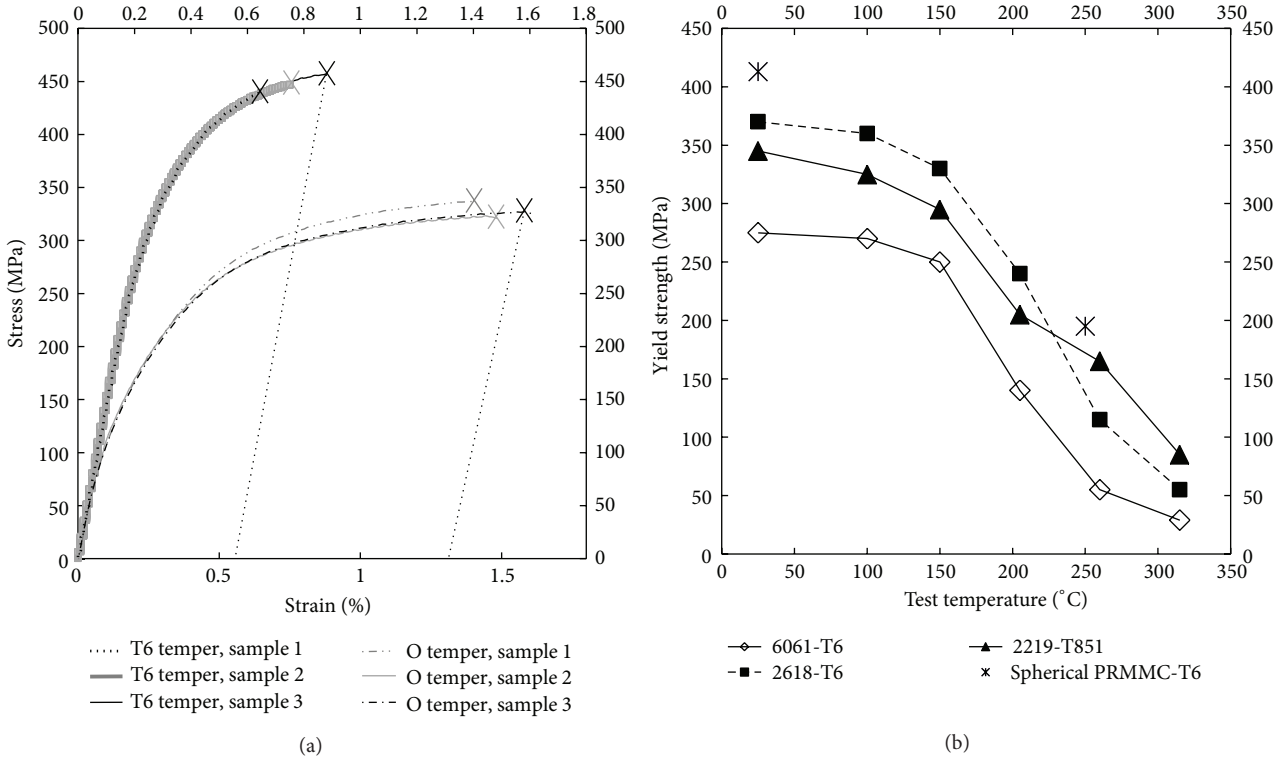

Figure 7: (a): Tensile curves of spherical PRMMC in T6 and O tempers at 25°C. (b) Yield strength evolution between 25°C and 315°C of AA6061 and high-temperature alloys AA2618 and AA2219 [11] as well as spherical PRMMC values at 25°C and 250°C. All >50°C data are after 1000 h ageing at the test temperature.

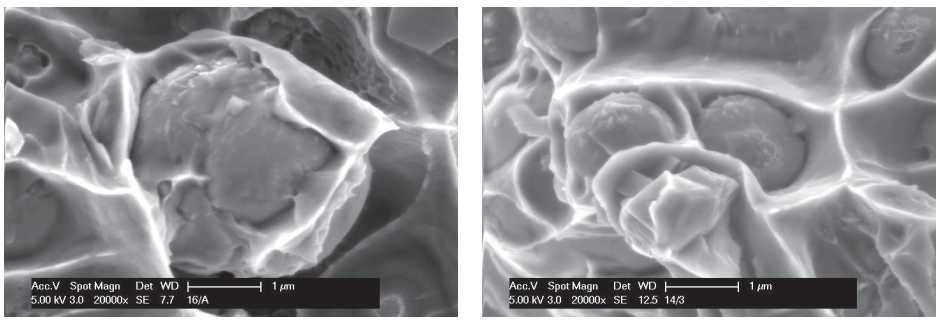

Figure 8: Fracture surfaces of the spherical PRMMC showing the tight bonding between the particles and the matrix. Magnification 20000x.

range of standard and low reinforced composites as illustrated in Figure 10. This is an encouraging result, although more trials and parameter exploration have to be done in order to come closer to VB = 0.3 mm.

Concerning the behavior of the composite during machining, the SEM image in Figure 12(a) shows that particles do not break and are not torn out whilst the tool insert removes the material. Cracks on the machined surface are not observed either. These observations confirm the positive effect of spherical particle shape on machining as explained by Harrigan [9]. The feed motion and the negative rake angle (Figure 11) produce compressive forces on the MMC. Under compression the spherical particles tend to be pushed and embedded into the matrix. The combination of the latter with the spherical particle effect allows such a high reinforced MMC to be machined without major surface damage and with limited tool insert wear.

Figure 12(b) shows the trace left by the tool insert on the machined surface. Differences in roughness can clearly be distinguished between region M and region N. Compression due to combination of feed motion and negative rake angle gives a smooth and void free surface in region M. The absence

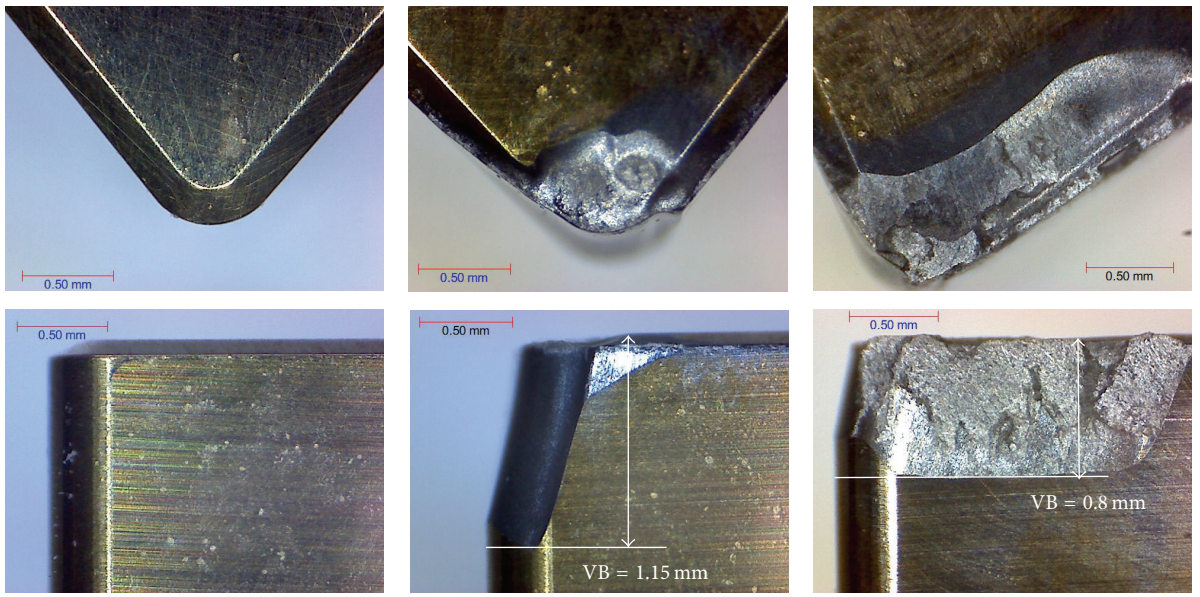

FIGURE 9: (a) New tool insert. (b) Worn tool insert after removing 50 cm^3 of material by turning, cutting depth = 0.5 mm. (c) Worn tool insert after removing 50 cm^3 of material by turning, cutting depth = 2 mm.

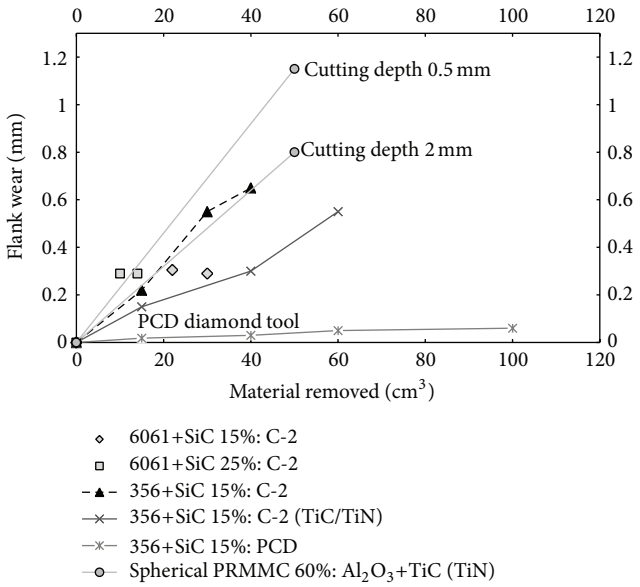

FIGURE 10: Al_2O_3+TiC (coated with TiN) insert flank wear after machining spherical PRMMC, comparison with five other MMCs [9], machined with noncoated carbide (C-2), TiC/TiN coated carbide, and PCD diamond inserts.

of compression from feed motion behind the cutting nose generates region N where voids are formed and some particles get less embedded than in region M.

This confirms the importance and the need of finishing machining to avoid the presence of these cavities, which represent potential crack initiation sites.

5. Conclusions

(i) Dissimilar behaviours are observed between standard alpha alumina and alpha-gamma-amorphous GAP alumina when used as reinforcement in AA6061 matrix alloy. Hardness tests at T4 and T6 tempers reveal that precipitation hardening is possible in GAP alumina reinforced 6xxx series aluminium alloys. This is because no reaction between magnesium and alumina happens during infiltration, solidification, or cooling of the composite. This behaviour is the opposite of what is observed with alpha alumina particles.

(ii) Tensile tests show that the ductility and strength tradeoff is only slightly below the critical threshold for applicability of the composites. In aerospace practice a minimum of 300–350 MPa for YS and 1% for elongation is required as a base line. In order to meet these targets an optimum temper/treatment or an alternative matrix has to be found.

(iii) Wear of tool inserts is very high when turning such highly reinforced composite. Nevertheless, adapted machining parameters combined with the spherical shape of the alumina particles allow being in the same range of wear of low volume fraction SiC particle reinforced aluminium composites.

(iv) Gas pressure infiltration processing offers the possibility to obtain pore-free near-net shape pieces with high elastic modulus. The combination of the latter with further improvements in composite design, postprocessing, and machining procedures may allow the application of highly reinforced MMCs and let

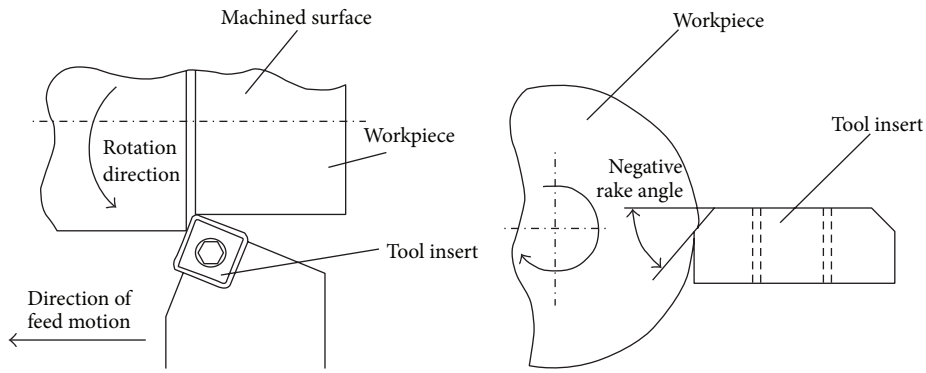

Figure 11: Schematic illustration of turning. (a) Top view. (b) Front view.

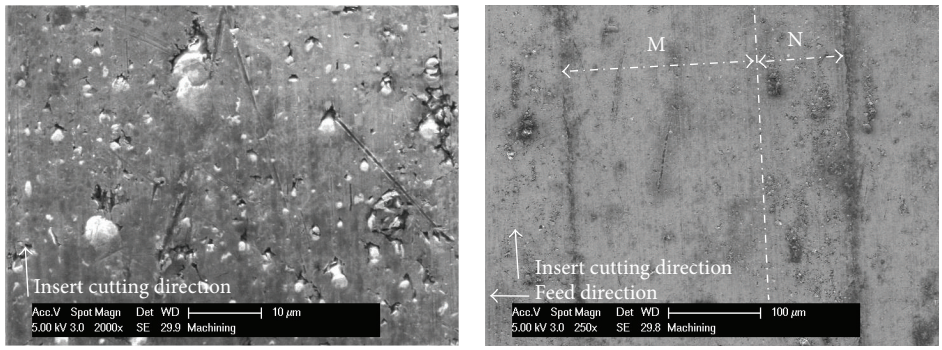

Figure 12: (a) SEM capture of machined surface, magnification 2000x. (b) SEM capture of machined surface divided in two regions. M: smooth and void-free surface and N: rough surface with cavities. Magnification 250x.

aerospace applications benefit from their high specific properties.

Conflict of Interests

The authors declare that there is no conflict of interests regarding the publication of this paper.

Acknowledgments

The authors would like to thank contributors from the Ecole Polytechnique Fédérale de Lausanne, that is, the Laboratory of Mechanical Metallurgy and the Mechanical Workshop of Material Science Institute ATMX for enabling the production and testing of the MMCs as well as Professor Andreas Mortensen for his expertise in the matter. Furthermore, Liebherr Aerospace is thanked for the high-temperature tensile tests and Dr. William Harrigan for the information on GAP powder and on machining of MMCs.

References

[1] C. Swift, "Metal matrix composites: the global market," Market Research Report, BBC Research, 2009.

[2] A. Mortensen, "Melt infiltration of metal matrix composites," in *Comprehensive Composite Materials, Volume 3: Metal Matrix Composites*, T. W. Clyne, Ed., chapter 3.20, pp. 521–554, Pergamon Press, New York, NY, USA, 2000.

[3] D. B. Miracle, "Metal matrix composites—from science to technological significance," *Composites Science and Technology*, vol. 65, no. 15-16, pp. 2526–2540, 2005.

[4] A. Miserez and A. Mortensen, "Fracture of aluminium reinforced with densely packed ceramic particles: influence of matrix hardening," *Acta Materialia*, vol. 52, no. 18, pp. 5331–5345, 2004.

[5] A. D. McLeod and C. M. Gabryel, "Kinetics of the growth of spinel, $MgAl_2O_4$, on alumina particulate in aluminum alloys containing magnesium," *Metallurgical Transactions A*, vol. 23, no. 4, pp. 1279–1283, 1992.

[6] S. Vaucher and O. Beffort, *Bonding and Interface formation in Metal Matrix Composites*, vol. 9, MMC-Assess Thematic Network, EMPA, 2001.

[7] J. C. Lee, K. N. Subramanian, and Y. Kim, "The interface in Al_2O_3 particulate-reinforced aluminium alloy composite and its role on the tensile properties," *Journal of Materials Science*, vol. 29, no. 8, pp. 1983–1990, 1994.

[8] W. C. Harrigan, "Machinable aluminium matrix composites," in *Proceedings of the Aeromat 2011 Presentation*, 2011.

[9] W. C. Harrigan, "Machinable aluminium matrix composite," in *Conference Proceedings: Commonality of Phenomena in Composite Materials II*, AIME, 2011.

[10] A. Evans, C. S. Marchi, and A. Mortensen, *Metal Matrix Composites in Industry: An Introduction and a Survey*, vol. 1, Kluwer Academic Publishers, 2003.

[11] J. G. Kaufman, *Properties of Aluminium Alloys: Tensile, Creep, and Fatigue Data at High and Low Temperatures*, AA & ASM International, 1999.

[12] Pechiney-Rhenalu, *Aluminium Semi-Finished Products*, Pechiney-Rhenalu, 1997.

[13] J. N. Hall, J. Wayne Jones, and A. K. Sachdev, "Particle size, volume fraction and matrix strength effects on fatigue behavior and particle fracture in 2124 aluminum-SiC_p composites," *Materials Science and Engineering A*, vol. 183, no. 1-2, pp. 69–80, 1994.

[14] D. A. Lukasak and D. A. Koss, "Microstructural influences on fatigue crack initiation in a model particulate-reinforced aluminium alloy MMC," *Composites*, vol. 24, no. 3, pp. 262–269, 1993.

[15] A. Awadallah and J. J. Lewandowski, "Forging of discontinuously reinforced aluminum composites," in *ASM Handbook, Volume 14A—Metalworking: Bulk Forming*, pp. 366–373, 2005.

[16] C. San Marchi, F. Cao, M. Kouzeli, and A. Mortensen, "Quasistatic and dynamic compression of aluminum-oxide particle reinforced pure aluminum," *Materials Science and Engineering A*, vol. 337, no. 1-2, pp. 202–211, 2002.

[17] V. P. Astakhov and J. P. Davim, "Tools (geometry and material) and tool wear," in *Machining: Fundamentals and Recent Advances*, pp. 29–57, 2008.